Available online at www.sciencedirect.com
SCIENCE DIRECT®
Journal of Photochemistry and Photobiology A: Chemistry 173 (2005) 99–105
Journal of Photochemistry and Photobiology A:Chemistry
www.elsevier.com/locate/jphotochem

# Photocatalytic activity of titania nanohole arrays

T. Hamaguchi*, M. Uno, S. Yamanaka

*Department of Nuclear Engineering, Graduate School of Engineering, Osaka University, Yamadaoka 2-1, Suita, Osaka 565-0871, Japan*

Received 25 May 2004; received in revised form 6 January 2005; accepted 12 January 2005
Available online 16 February 2005

**Abstract**

Titania nanohole array with various hole diameters was obtained by liquid phase deposition (LPD) method. Photocatalytic activity of titania nanohole arrays was estimated by the photodecomposition properties of acetaldehyde and methylene blue. The photodecomposition rates of methylene blue and acetaldehyde were increased with heat treatment temperature. Titania nanohole array sintered at 1173 K showed the highest photocatalytic activity. This result was caused by the fact that the crystallinity increased with heat treatment temperature and the specific surface area of titania nanohole array was almost constant with heat treatment. The sample with the 250 and 200 nm diameter showed the highest photocatalytic activity.


*Keywords:* Photocatalyst; Anodic alumina; Liquid phase deposition method

## 1. Introduction

Titania has a high potential for many industrial applications and therefore many researches focus on its fabrication and characterization [1–5]. In recent years, major attention has been devoted to its ability of photocatalysis [6]. Much effort has been made to prepare titania with a large specific surface area in order to increase the photocatalytic activity. In our previous reports [7,8], we have described a new process for synthesis of titania nanohole array with a large specific surface area.

In this process, we use a liquid phase deposition (LPD) method with an anodic alumina as a starting material. The LPD method is a novel wet process, which has been developed for the preparation of metal oxide thin films [9–14]. In this process, it is possible to produce thin metal oxide films or hydroxide films directly on a substrate that is immersed in a treatment solution for deposition. Metal oxide or hydroxide thin films are formed by means of both a hydrolysis equilibrium reaction of a metal-fluoro complex ion and an $F^-$ consuming reaction of boric acid or aluminum metal, which acts as a scavenger for $F^-$ [9]. The hydrolysis reaction of metal-fluoro complex ions [$MF_x^{(x-2n)-}$], in the treatment solution for deposition is given as follows:

$$MF_x^{(x-2n)-} + nH_2O \Leftrightarrow MO_n + xF^- + 2nH^+ \quad (1)$$

The equilibrium reaction (1) is shifted to the right-hand side by the addition of boric acid or aluminum metal, which readily reacts with the $F^-$ ions to form stable complex ions (Eqs. (2) and (3)):

$$H_3BO_3 + 4H^+ + 4F^- \Leftrightarrow BF_4^- + H_3O^+ + 2H_2O \quad (2)$$

$$Al + 6H^+ + 6F^- \Leftrightarrow H_3AlF_6 + 3/2(H_2) \quad (3)$$

The LPD method is a very simple process and does not require any special equipment such as a vacuum system. It can, moreover, be applied readily to the preparation of thin films on various types of substrates with large surface areas and complex morphologies, since the LPD is performed in an aqueous solution. In our new process [7,8], since we use anodic alumina as a scavenger and starting template material, we can synthesize the oxide nanohole array in a single process. In this study, we measured the photocatalytic activity

* Corresponding author. Tel.: +81 6 6879 7905; fax: +81 6 6879 7889.
*E-mail address:* thama@stu.nucl.eng.osaka-u.ac.jp (T. Hamaguchi).

1010-6030/$ – see front matter © 2005 Elsevier B.V. All rights reserved.
doi:10.1016/j.jphotochem.2005.01.008

Table 1
Sample name and the reaction condition for the sample

| Sample name | Reaction time (h) | Amount of titania (mg) | Ti/Ti + Al (wt.%) | Hole diameter (nm) |
|---|---|---|---|---|
| Ti-05 | 0.5 | 8.7 | 2.8 | 300 |
| Ti-10 | 1.0 | 45 | 14.2 | 250 |
| Ti-15 | 1.5 | 78 | 23.1 | 200 |
| Ti-20 | 2.0 | 110 | 31.6 | 150 |

for titania nanohole array of photodecomposition of acetaldehyde gas and methylene blue.

## 2. Experimental

The ammonium hexafluorotitanate ($(NH_4)_2TiF_6$; Aldrich Inc.) was dissolved at a concentration of 0.1 mol/dm$^3$ in distilled water as the treatment solution 1 to synthesize the titania nanohole arrays. Anodic alumina disks (anodisc; WHATMAN Ltd.) were used as the starting material and $F^-$ scavenger. The disk diameter and thickness of the anodic alumina were 13 mm and 50 μm, respectively. The anodic alumina was immersed in the treatment solution 1 and the reaction was carried at 293 K. For comparison of the photocatalytic activity, titania film was prepared by LPD method. The ammonium hexafluorotitanate and boric acid were dissolved at a concentration of 0.1 mol/dm$^3$ in distilled water as the treatment solution 2 for deposition of thin film. Soda lime glass used as substrates was immersed in the treatment solution and the reaction was carried at 20 °C for 24 h. The sample was then removed from the treatment solution, washed with distilled water and acetone and dried at room temperature. Heat treatments of the deposited films were carried out in airflow for 1 h at temperatures ranging from 373 to 1373 K. The sample name, the reaction time for the preparation of the sample, the amount of titania, and the titanium content in weight are described in Table 1.

The surface morphologies and cross-section of the anodic alumina disk and the titania nanohole array were observed by field-emission scanning electron microscopy (FE-SEM) (JEOL, JSM-6700F). The BET surface area was determined by $N_2$ adsorption (YUASA-IONICS COMPANY, AUTOSORB). Photodecomposition experiment of acetaldehyde vapor was carried out as follows: the sample with 25 cm$^2$ apparent surface area was placed at the bottom of a quartz glass cell (volume, 500 ml). The air in the cell was replaced by a gas consisting of a 4:1 mixture of $N_2$ and $O_2$ and containing 50% humidity. Then, acetaldehyde was added to the cell to give an initial concentration of 100 ppm. After 30 min, irradiation was commenced. A black light, whose wavelength was about 300–420 nm, was used as the light source. The light intensity was 1.0 mW/cm$^2$ at the bottom of the reaction cell, as measured by a detector with a wavelength detection range of 320–380 nm. The 0.50 dm$^3$ gas in the reaction cell was then removed using a gas syringe at periodic intervals for gas chromatography. Photodecomposition of methylene blue was carried out as follows: the sample of 13 mm diameter was immersed in the 0.1 mmol/dm$^3$ methylene blue solution for 1 h. Then, the sample was removed from the methylene blue solution and dried in a dark place at room temperature. The decomposition properties of methylene blue were estimated by the delta absorbance (Eq. (4)), the wavelength of which was 650 nm as measured by PCC-2 (ULVAC Inc.).

$$\Delta ABS = ABS_{\dagger} - ABS_{initial} \quad (4)$$

$ABS_{\dagger}$ is the absorbance at various illumination times and $ABS_{initial}$ the absorbance at initial time.

## 3. Results and discussion

Fig. 1 shows FE-SEM photographs of the surface structure of anodic alumina as the starting material, Ti-05, Ti-10, Ti-15, and Ti-20. Anodic alumina in Fig. 1(a) had many pores whose mean diameter was approximately 200 nm. From Fig. 1(b), we can observe a structure similar to that of the anodic alumina. The hole diameter of Ti-05 is about 300 nm. It could be seen that the widening of hole diameter was caused by the dissolution of anodic alumina. The surface structure of Ti-10 (Fig. 1(c)), Ti-15 (Fig. 1(d)), and Ti-20 (Fig. 1(e)) had many tubes and the inside diameters of the sample were about 250, 200, and 150 nm, respectively. The outside diameter of these samples was almost the same, approximately 300 nm. The wall thickness values of these samples were 30, 50, and 70 nm, respectively. The distance between each tubule decreased when the reaction time was increased and there was no scaffold formed by the wall of anodic alumina [8] in Fig. 1(d) and (e).

Fig. 2 shows FE-SEM photographs of the cross-sectional structure of Ti-05, Ti-10, Ti-15, and Ti-20. We could not confirm whether titania exists on the surface structure of Ti-05 (Fig. 1(a)), however, we could observe titania particles on the wall of anodic alumina from the cross-sectional view of Ti-05 (Fig. 2(a)). The remaining anodic alumina was observed between the tubes (Fig. 2(b) and (c)). Comparing these figures, the scaffolds formed from anodic alumina could be observed over the top of titania tubes in Fig. 2(b), however, no scaffolds could be observed in Fig. 2(c) and only anodic alumina between tubes was observed. This result agrees with the FE-SEM analysis of the surface morphologies. There remained no anodic alumina in Fig. 2(d). It is found that Ti-20 consisted of only titania of at least 7 μm from the surface.

The following part of the study demonstrates how some properties of titania nanohole array changed with heat treatment temperature. Fig. 3 shows X-ray diffraction patterns for the titania nanohole array sintered at various temperatures. The titania nanohole array samples as prepared and sintered up to 673 K showed no peaks, while the titania nanohole array sintered at and over 773 K showed some peaks. For titania nanohole array sintered below 973 K, diffraction peaks other than that of anatase $TiO_2$ were not observed. The diffraction

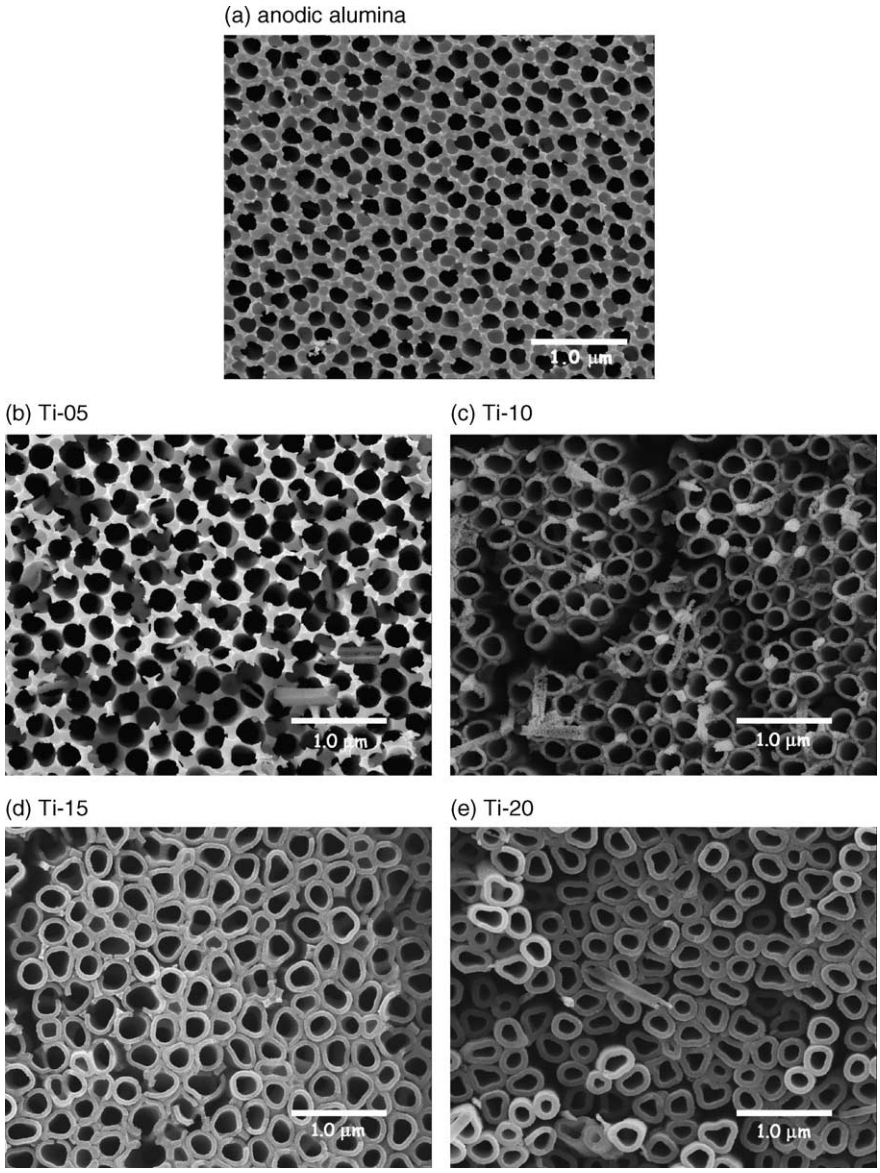


Fig. 1. FE-SEM photographs of the surface structure of titania nanohole arrays synthesized for various reaction times.

peaks of rutile of titania appeared for titania nanohole array sintered above 1373 K. The ratio of anatase to rutile was calculated as 85:15 from this peak. Fig. 4 shows the specific surface area of Ti-10 sintered at various temperatures. The specific surface area of non-heat treatment Ti-10 was 28.90. The specific surface area is calculated by dividing the total surface area by the sum of the weights of titania and remaining alumina. The specific surface area of titania nanohole array was almost constant up to 1173 K. We consider that this was due to the structure of titania nanohole array with anodic alumina. Neither the structure of the anodic alumina nor that of the titania nanohole array changed with heat treatment up to this temperature. The sample sintered at 1373 K, however, could not keep the structure because of the anatase to rutile phase transition of titania as shown in Fig. 5. So the photocatalytic activity of the sample sintered at 1373 K was lower than that at 1173 K.

Fig. 6 shows the photodecomposition properties of the acetaldehyde by using Ti-10 sintered at various temperatures. The sample sintered at up to 573 K hardly decomposed the acetaldehyde gas. The samples sintered at above 973 K decomposed the acetaldehyde gas faster than that sintered at 773 K, and the highest photocatalytic activity was attained with the sample sintered at 1173 K. Since the purpose behind the photodecomposition properties of acetaldehyde is the deodorization, we have to estimate not only the decomposition rate of acetaldehyde but also the generation rate of carbon dioxide. Fig. 7 shows the generation properties of carbon dioxide by the titania nanohole array sintered at above 773 K. In this figure, the amount of generated carbon diox-

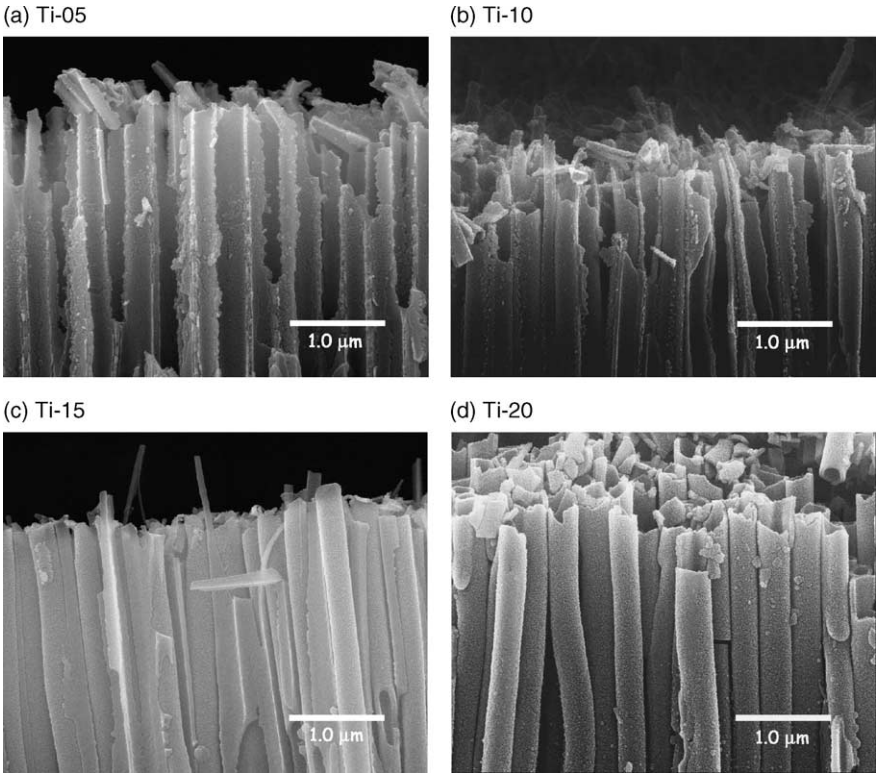


Fig. 2. FE-SEM photographs of cross-sectional structure of titania nanohole arrays synthesized for various reaction times.

ide is set to be zero at 30 min. The lowest generation rate of carbon dioxide was shown by Ti-10 sintered at 773 K. The generation rate of carbon dioxide by the sample sintered at 1173 K was slightly higher than that at 973 K. These results show that the photooxidation power of the sample sintered at 1173 K was the strongest. The reason behind the highest photocatalytic activity of the titania nanohole is discussed as follows. We focused on two factors: one is the crystallinity and the other is specific surface area. The crystallinity of titania nanohole array became higher with heat treatment temperature (from Fig. 3). On the other hand, the specific surface area was almost constant with heat treatment temperature up to 1173 K (from Fig. 4). From these results, it can be concluded that the highest photocatalytic activity was caused by the highest crystallinity of the sample sintered at 1173 K. The reason why titania nanohole array sintered at 1373 K showed

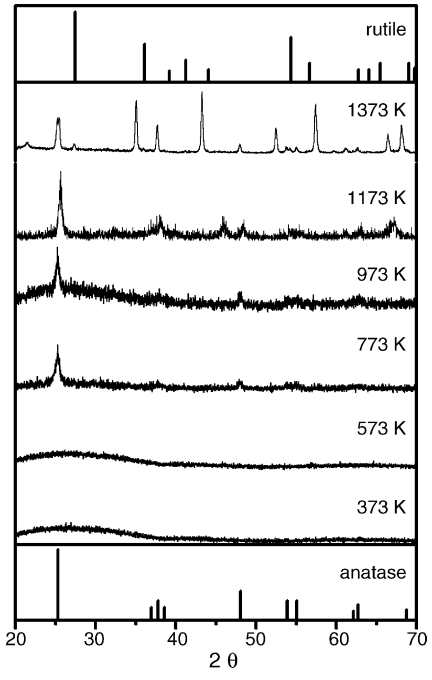


Fig. 3. XRD properties of titania nanohole arrays sintered at various temperatures.

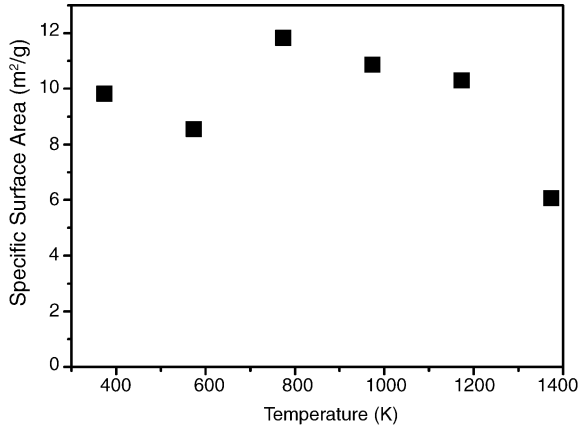


Fig. 4. Specific surface area of the Ti-10 sintered at various temperatures.

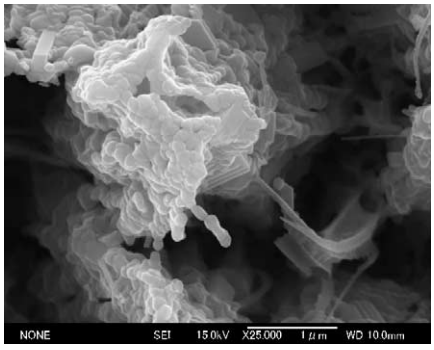


Fig. 5. FE-SEM photograph of the surface structure of titania nanohole array sintered at 1373 K.

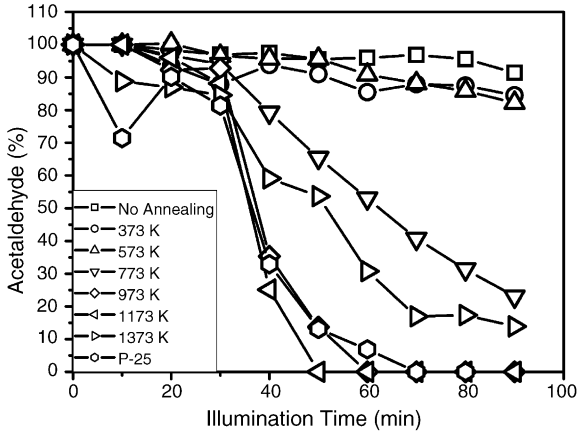


Fig. 6. Photodecomposition properties of acetaldehyde by using Ti-10 sintered at various temperatures.

lower photocatalytic activity than that sintered at 1173 K was that the sample sintered at 1373 K showed rutile phase, which demostrated lower photocatalytic activity than anatase phase and had lower specific surface area than the sample sintered at 1173 K.

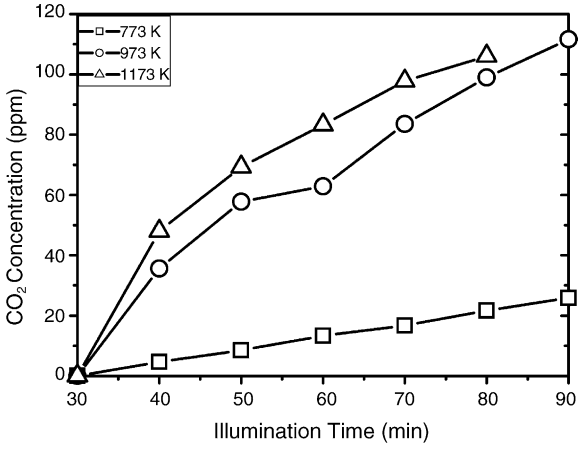


Fig. 7. Photogeneration properties of carbon dioxide by using Ti-10 sintered at various temperatures.

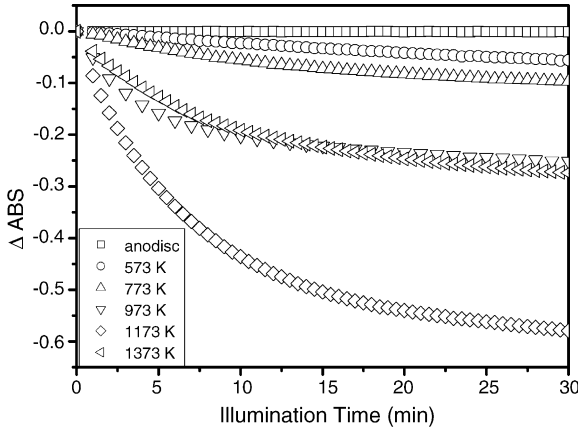


Fig. 8. Photodecomposition properties of methylene blue by using Ti-10 sintered at various temperatures.

Fig. 8 shows the photodecomposition properties of methylene blue by using Ti-10 sintered at various temperatures. As a reference, the photodecomposition properties of methylene blue by using anodic alumina. Ti-10 sintered at 573 K and anodic alumina hardly decomposed methylene blue, however, Ti-10 sintered at 773 K could decompose methylene blue. This tendency was the same as the photodecomposition properties of acetaldehyde gas. This tendency was the same as the photodecomposition properties of the acetaldehyde gas. These results can be related to the result of X-ray diffraction (Fig. 3). In other words, titania nanohole array, which has low crystallinity does not show the photocatalytic activity. Above 573 K annealing leads to an increase of crystallinity and hence the rise of photocatalytic activity.

According to a previous report [15], titania thin films prepared by LPD method show that the photocatalytic activity, and the highest photodecomposition property of acetaldehyde were achieved by the thin film sintered at 573 K. Fig. 9 shows the photodecomposition properties using methylene blue of titania thin films prepared by LPD method sintered in the present study. We found that the thin film sintered at 573 K and the sample sintered at 773 K showed the highest pho-

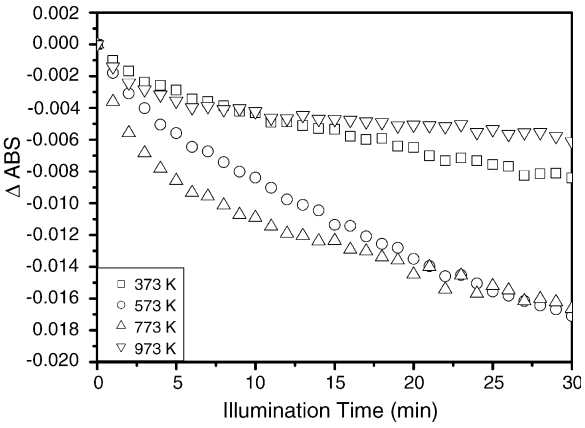


Fig. 9. Photodecomposition properties of methylene blue by using titania thin film by LPD method sintered at various temperatures.

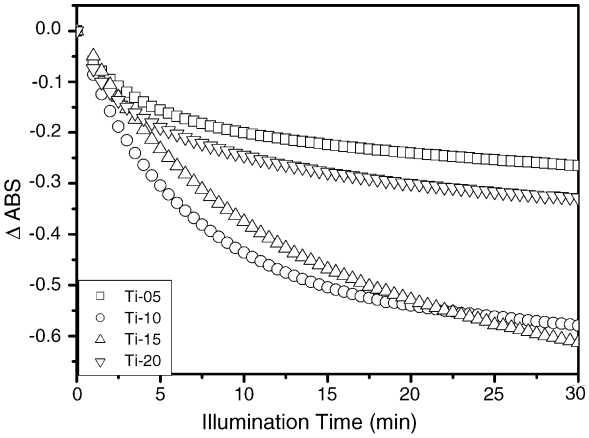


Fig. 10. Photodecomposition properties of methylene blue by various sample sintered at 1173 K.

todecomposition property of methylene blue. However, the titania nanohole array, Ti-10 asprepared and sintered below 573 K, showed no photocatalytic activity. We concluded that Ti-10 thin films as-prepared showed no photocatalytic activity due to the presence of Al ions. According to Gesenhues [16], photocatalytic activity of Al-doped titania was lower than that of non-Al-doped titania. Because of using Al ion as an $F^-$ scavenger, the titania nanohole array included Al ion as well as titania particles and showed low photocatalytic activity after heat treatment at low temperatures.

Fig. 10 shows the photodecomposition properties of methylene blue using various hole diameter samples sintered at 1173 K. Both Ti-05 and Ti-10 showed the lowest photodecomposition rate of methylene blue. Ti-10 and Ti-15 showed a very high photodecomposition rate. The reason for the high photocatalytic activity might be that Ti-10 and Ti-15 included larger amount of titania powder than Ti-05 as shown in Table 1. Although Ti-20 included larger amount of titania powder than Ti-10 and Ti-15, it showed low photocatalytic activity. Fig. 11 shows the specific surface area of Ti-10, Ti-15 and Ti-20 sintered at 1173 K. In this figure, open mark shows the specific surface area of these samples calculated by dividing the total surface area by the weights of titania and remaining alumina, and solid mark shows the specific surface area of the titania calculated by dividing the total surface area by the sum of weights of only titania. The specific surface area of the samples was almost constant, however, the specific surface area of the titania decreased with reaction time. So, we concluded that the photocatalytic activity of Ti-20 was lower than that of Ti-10 and Ti-15. However, it is impossible to justify that the photocatalytic activity of Ti-10 was similar to that of Ti-15. Therefore, we considered other possibilities for this result. We expected that when the hole diameter decreased the depth of photoillumination became less. However, we are forced to conclude that we do not have any definite answers to this question. Further systematic experiments on variation of the photocatalytic activity with hole diameter and the sample thickness are needed.

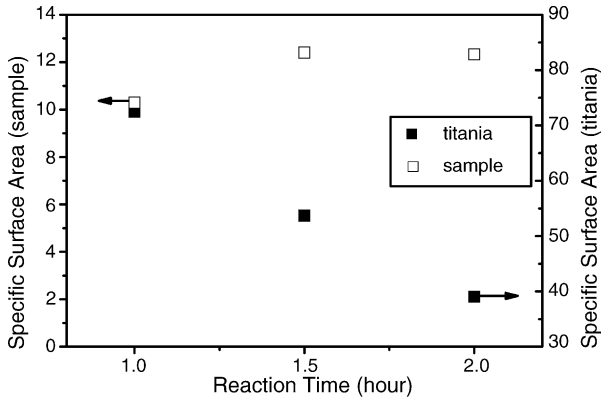


Fig. 11. Specific surface area of the sample prepared for several reaction time.

## 4. Conclusions

Photocatalytic activity of titania nanohole arrays was estimated by the photodecomposition properties of methylene blue and acetaldehyde. The activity of photodecomposition of methylene blue and acetaldehyde was increased with heat treatment temperature. Titania nanohole array sintered at 1173 K showed the highest photocatalytic activity. This result was caused by the fact that the crystallinity increased with heat treatment temperature and the specific surface area of titania nanohole array was almost constant with heat treatment. Titania nanohole array with various hole diameters was prepared. The samples with 250 and 200 nm diameters showed the highest photocatalytic activity.

## Acknowledgements

The present study has been partially supported by the Ministry of Education, Hosokawa Powder Technology Foundation, Kansai Research Foundation for Technology Promotion, the Kazuchika Okura Memorial Foundation, the Kurata Memorial Hitachi Science and Technology Foundation, Hyogo Science and Technology Association, the Foundation of Ando Laboratory, the Murata Science Foundation, and Steel Industry Foundation for the Advancement of Environmental Protection Technology. The author is also deeply indebted to Kanagawa Academy of Science and Technology for their considerable assistance with the photodecomposition experiment of acetaldehyde.

## References

[1] P. Zeman, S. Takabayashi, Thin solid Films 433 (2003) 57.
[2] S. Schiller, G. Beister, W. Sieber, G. Schirmer, E. Hacker, Thin Solid Films 83 (1981) 239.
[3] L.M. Williams, D.W. Hess, J. Vac. Sci. Technol. A 1 (1983) 1810.

[4] N. Martin, C. Rousselot, C. Savall, F. Palmino, Thin Solid Films 287 (1996) 154.
[5] N. Negishi, K. Takeuchi, T. Ibusuki, Appl. Surf. Sci. 121–122 (1997) 417.
[6] A. Fujishima, K. Honda, Nature 238 (1972) 37.
[7] S. Yamanaka, T. Hamaguchi, H. Muta, K. Kurosaki, M. Uno, J. Alloys Compd. 373 (2004) 312–315.
[8] T. Hamaguchi, M. Uno, S. Yamanaka, J. Alloys Compd. 386 (2005) 265–269.
[9] A. Hishinuma, T. Goda, M. Kitaoka, S. Hayashi, H. Kawahara, J. Surf. Sci. 48–49 (1991) 405–408.
[10] S. Deki, Y. Aoi, O. Hiroi, A. Kajinami, Chem. Lett. 1996 (1996) 433–434.
[11] S. Deki, Y. Aoi, J. Okibe, H. Yanagimoto, A. Kajinami, M. Mizuhata, J. Mater. Chem. 7 (1997) 1769–1772.
[12] H.Y.Y. Ko, M. Mizuharta, A. Kajinami, S. Deki, J. Mater. Chem. 12 (2002) 1495–1499.
[13] K. Tsukuma, T. Akiyama, N. Yamada, H. Imai, J. Non-Cryst. Solids 231 (1998) 161–168.
[14] K. Tsukuma, T. Akiyama, H. Imai, J. Non-Cryst. Solids 210 (1997) 48–54.
[15] H. Kishimoto, K. Takahama, N. Hashimoto, Y. Aoi, S. Deki, J. Mater. Chem. 8 (9) (1998) 2019.
[16] U. Gesenhues, J. Photochem. Photobiol. A: Chem. 139 (2001) 243.